Progress In Electromagnetics Research M, Vol. 45, 59–71, 2016

Mathematical Analysis and Modeling of Single-Walled Carbon Nanotube Composite Material for Antenna Applications

Yaseen N. Jurn[1, *], Mohd F. Malek[2], and Hasliza A. Rahim[1]

Abstract—In this paper, the mathematical analysis of a single-walled carbon nanotube composite material (SWCNT-composite) is presented in order to estimate its effective conductivity model and other important parameters. This composite material consists of SWCNT coated by other different materials. The effects of the radius of SWCNT and average thickness of coating layer on this effective conductivity model are investigated. The effects of using different types of coating materials with different radii of SWCNTs on the behavior of this composite material are also presented. An investigation of electromagnetic properties of SWCNT-composite material was carried out based on designing and implementing the dipole antenna configuration using a common electromagnetic engineering tool solver CST (MWS). The results obtained from comparisons between SWCNT and SWCNT-composite materials are presented, based on their electromagnetic properties.

1. INTRODUCTION

The carbon nanotubes (CNTs) have been used in many applications, especially in the design of different types of sensors [1–4], due to their unique properties. The original structure of CNTs is a graphene sheet wrapped in order to configure a cylinder with the nanometers radius of scale dimension and some centimeters in length. Based on their tubular structure, the CNTs can be considered as a metallic or semiconducting material [5]. The number of tubes that constructs the CNTs was adopted to classify the CNTs into SWCNTs and multi-walled carbon nanotubes (MWCNTs) [6, 7]. SWCNTs consist of one cylinder, whereas MWCNTs consist of several concentric cylinders. Previous studies emphasized the investigation universal techniques in order to predict EM properties of the SWCNT, based on the design of the SWCNT dipole antenna configuration [6, 8–14]. In this work, the metallic armchair SWCNT was therefore adopted.

Indeed, CNTs-composite materials are widely applied in the area of material sciences. CNTs-composite materials are constructed, based on two approaches to obtain new materials with improved properties. The first approach depends on synthesis of CNTs with other materials through different chemical procedures, in order to construct new materials based-CNTs [15–19]. Meanwhile, the second approach depends on coating CNTs (SWCNTs and MWCNTs) by other materials, in order to improve the surfaces properties of CNTs. The coating approach is, in fact, one of the fabrication approaches used for handling the surface problems of CNTs. This approach is also applied to produce a good candidate materials utilized in various areas of sciences including biosensors, semiconductors, electrochemical sensors, microelectrodes, nanowire, and biomedicine. These new composite materials have upscale properties and can be fabricated by coating CNTs with various materials. To date, miscellaneous SWCNT-composite materials have been successfully produced from depositing the nanoparticles of metallic, semiconducting and insulating materials onto the surface of SWCNTs using different coating

Received 17 September 2015, Accepted 9 November 2015, Scheduled 18 December 2015

* Corresponding author: Yaseen Naser Jurn (yaseen_nasir@yahoo.com).

[1] School of Computer and Communication Engineering, University Malaysia Perlis (UniMAP), Perlis, Malaysia. [2] School of Electrical System Engineering, University Malaysia Perlis (UniMAP), Perlis, Malaysia.

methods [20–22]. The main target of coating approach is to improve the electrical and mechanical properties of the new SWCNT-composite materials. Also, several methods were implemented for coating the multi-walled CNTs (MWCNTs) and SWCNTs [21, 23–27]. Hence, the SWCNT-composite structure will be adopted and analyzed in this work.

This paper aims to present the mathematical analysis for SWCNT-composite material structure consisting of SWCNT, coated by other materials. In this analysis, the effective conductivity model and other key parameters for SWCNT-composite material are introduced. The dependence of these parameters on the radius of SWCNTs, an average thickness of coating layer and the conductivity of various types of coating material were also investigated. In this study, the mathematical analysis model was used to present an efficacious modeling approach for SWCNT-composite material, in order to estimate the electromagnetic properties of this material. The SWCNT-composite dipole antenna configuration is employed for this purpose.

2. METHODOLOGY

In this section, the work progress is presented as follow: First, the simple modeling approach for SWCNT is presented for the purpose of compression with SWCNT-composite material. Second, the efficacious electromagnetic (EM) modeling approach for the (SWCNT-composite) material is proposed, based on the mathematical analysis of this material. Finally, the required mathematical analysis which aims to provide evidence for this work is also presented in this paper.

2.1. Modeling of SWCNT

To overcome the difficulty in dealing with the hollow cylinder of SWCNT, a solid cylinder model was adopted to represent the SWCNT. The transformation factor TRF between these structures was presented in previous works [6, 28]. In the current work, the nano-solid tube material (NSTM) model is presented to model the SWCNT. The raw material of NSTM is the original material of SWCNT. This modeling approach aims to predict the EM properties of SWCNT through designing the SWCNT dipole antenna in the CST (MWS) software package. The conductivity of the NSTM model is deduced from the surface conductivity of SWCNT (σ_{SWCNT}) given by Equation (2) [6], as shown in the formula below:

$$\sigma_{NSTM} = \left(\frac{2}{r}\right)\sigma_{SWCNT} = -j\frac{4e^2V_f}{\pi^2hr^2(w-jv)} \tag{1}$$

$$\sigma_{SWCNT} = -j\frac{2e^2V_f}{\pi^2hr(w-jv)} \tag{2}$$

where, e is the electron charge, r the radius of SWCNT, h the reduced Plank's constant ($h = 1.05457266 \times 10^{-34} J \cdot s$), V_f the Fermi velocity of CNT ($V_f = 9.71 \times 10^5$ m/s), v a phenomenological relaxation frequency ($v = {}^{6T}/_{r}$), so, $F_v = {}^{v}/_{2\pi}$ where ($T = 300$) is temperature in kelvin, and w is the angular frequency.

The radius of SWCNT was computed by this formula ($r = \frac{\sqrt{3}}{2\pi}b\sqrt{m^2+mn+n^2}$), where ($m$ and n) are integers, and $b = 0.142$ nm is the interatomic distance in graphene. The radius of SWCNT depends on the dual indexes (m, n) which are adopted to characterize the SWCNT into different types such as armchair, zigzag, and chiral [6]. The armchair metallic SWCNT at ($m = n$) is adopted in this work.

The plasma frequency (w_{psw}) of the SWCNT is estimated, based on the bulk conductivity model presented in [6], and the relative complex permittivity of the SWCNT (ε) is estimated as follows

$$w_{psw} = \frac{2e}{\pi r}\sqrt{\frac{V_f}{\varepsilon^o h}} \tag{3}$$

$$\varepsilon' = 1 - \frac{w_{psw}^2}{w^2+v^2} \tag{4}$$

$$\varepsilon'' = \frac{vw_{psw}^2}{w^3+wv^2} \tag{5}$$

where (ε') is the real part and (ε'') the imaginary part of the SWCNT relative complex permittivity. Hence, in order to implement the simulation technique of this modeling approach, the material parameters of the SWCNT are inserted in the CST (MWS) as a new normal.

2.2. Mathematical Analysis of SWCNT-Composite Material

The SWCNTs composite material adopted in this work is composed of SWCNT coated by a thin layer of another material. This structure leads to building and constructing a new thick rod, as illustrated in Figure 1. The new rod is characterized by properties different from those of its original materials (SWCNT and coating material).

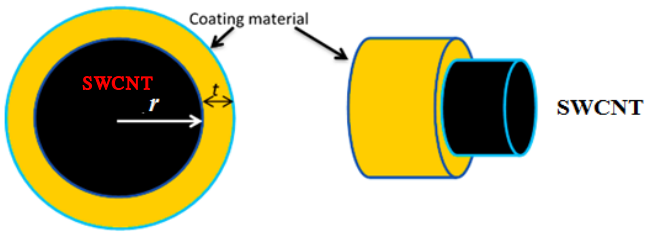

Figure 1. Structure of SWCNT-composite material (SWCNT coated by another material).

In order to predict the EM properties of SWCNT-composite material, the mathematical analysis of important parameters for this material was conducted. These parameters acclimate the SWCNT-composite material with CST (MWS) software package. The effective electrical conductivity plays a key role in the electrical properties of the SWCNT-composite material. Therefore, estimating the effective conductivity model of this composite material is very necessary for modeling and simulating this composite material in the CST (MWS) software package. The effective conductivity model of the SWCNT-composite material is described in this section.

In this work, the effective conductivity of the SWCNT-composite material is given by ($\sigma_{composite}$), and the conductivity of coating material is symbolized by (σ_{coat}). Based on the principle of deriving the mathematical model of the effective conductivity for the MWCNT structure, as presented in [7], the mathematical model of the effective conductivity of SWCNT-composite material is derived as follows:

$$\sigma_{composite} = \sum_{j=1}^{k} m_j \sigma_{zj} \tag{6}$$

where, k is the number of materials that constructs the composite material. In this work, ($k = 2$) represents SWCNT and coating materials. Then,

$$\sigma_{composite} = \sum_{j=1}^{2} m_j \sigma_{zj} = m_1\sigma_{z1} + m_2\sigma_{z2} \tag{7}$$

m_j is the volume fraction factor of the material, (σ_{z1}) the conductivity of SWCNT (σ_{SWCNT}), and (σ_{z2}) the conductivity of coating material (σ_{coat}). As a result, the effective conductivity model of the SWCNT-composite material is derived, as given by

$$\sigma_{composite} = P\sigma_{SWCNT} + A\sigma_{Coat} \tag{8}$$

Based on the original structure of SWCNT (hollow cylinder), P is the circumference of SWCNT ($P = 2\pi r$) and A the average radial cross-section area of coating layer depending on the average thickness of coating layer (t). Then, by substituting Equation (2), the final formula of the effective conductivity model for SWCNT-composite material is demonstrated by the formula below

$$\sigma_{composite} = \frac{1}{(r+t)^2}\left[-j\frac{4e^2V_f}{\pi^2 h(w-jv)} + t^2\sigma_{Coat}\right] \tag{9}$$

In addition to the effective conductivity model of the SWCNT-composite material, the plasma frequency is considered as a remarkable parameter for the purpose of EM modeling and simulation of this composite material in CST (MWS) software package for antenna applications. Based on the effective conductivity model mentioned in Equation (9) and the bulk conductivity model presented in [6], the plasma frequency of SWCNT-composite material ($W_{P,composite}$) is deduced as follows:

$$W_{P,composite} = \frac{e}{\pi(r+t)}\left[\frac{4V_f + \pi^2 hM}{h\varepsilon^o}\right]^{1/2} \tag{10}$$

$$M = \left(\frac{t^2 v\sigma_{Coat}}{e^2}\right) \tag{11}$$

At the same time, the phenomenological relaxation frequency of SWCNT-composite material ($v_{compsite}$) is estimated by a formula below based on the basic mathematical definition of this parameter presented previously [7].

$$v_{composite} = \frac{6T}{(r+t)} \tag{12}$$

where T is temperature in kelvin. The conductivity model of the coating material used in this work is the standard conductivity formula of materials presented in previous research [29].

$$\sigma_{coat} = \frac{e^2 N_{coat}^D}{2m_e v_{coat}} \tag{13}$$

where $v_{coat} = {}^1/_{\tau_{rlxcoat}}$, at $\tau_{rlxcoat}$ is the relaxation time of coating material. N_{coat}^D is the number of electrons per (m^3) of coating material. These parameters (N_{coat}^D, v_{coat}) are useful for distinguishing the materials from others.

On the other hand, the real part ($\varepsilon'_{c,composite}$) and imaginary part ($\varepsilon''_{c,composite}$) of the relative complex permittivity ($\varepsilon_{c,composite}$) of the SWCNT-composite material are presented based on the plasma frequency

$$\varepsilon'_{c,composite} = 1 + \frac{W_{P,compsite}^2}{w^2 + v_{compsite}^2} \tag{14}$$

$$\varepsilon''_{c,composite} = \frac{v_{compsite} W_{P,composite}^2}{w^3 + w v_{compsite}^2} \tag{15}$$

In another context, according to the general admitted definition of the complex permittivity demonstrated in previous research [29], the permittivity and conductivity of the SWCNT-composite material are given by the following relation

$$\varepsilon_{c,composite} = 1 + \frac{\sigma_{composite,i}}{w\varepsilon^o} - j\frac{\sigma_{composite,r}}{w\varepsilon^o} \tag{16}$$

$$\varepsilon'_{c,composite} = 1 + \frac{\sigma_{composite,i}}{w\varepsilon^o} \tag{17}$$

$$\varepsilon''_{c,composite} = \frac{\sigma_{composite,r}}{w\varepsilon^o} \tag{18}$$

Hence, the relative complex permittivity of SWCNT-composite material is modeled with either Equations (14) and (15) or Equations (17) and (18), where both equation sets provide the same results. Therefore, the EM parameters of SWCNT-composite material extracted (or estimated) in this work is utilized to represent this composite material in different 3D EM simulation software packages including CST (MWS), HFSS and others.

2.3. Simulation Modeling of SWCNT-Composite Material

In this section, the simulation of the equivalent modeling approach for SWCNT-composite material is illustrated. In order to predict the EM properties of the SWCNT-composite material, the mathematical

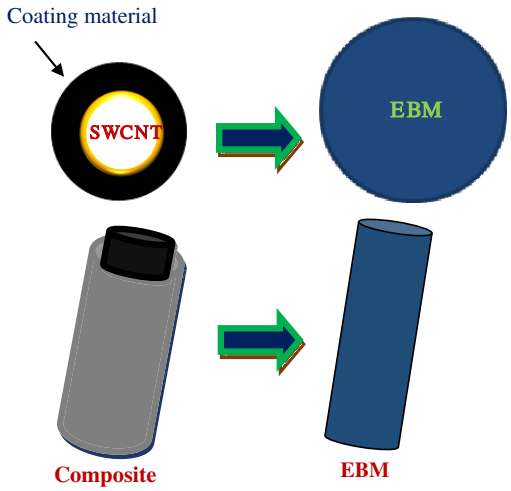

Figure 2. EBM model structure of SWCNT-composite material. Left side is the SWCNT-composite material and right side is the EBM model.

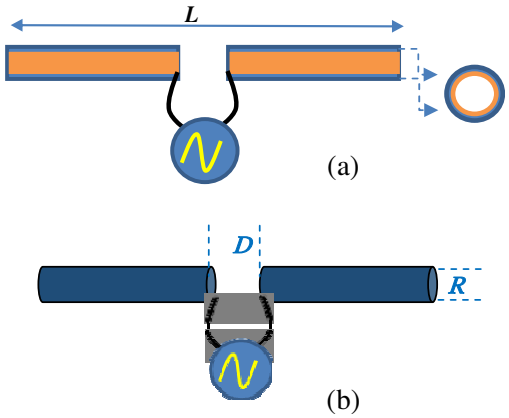

Figure 3. Design of (a) SWCNT-composite dipole antenna, and (b) EBM-dipole antenna with center feed gap.

analysis is presented in this work. The core parameters of this material were utilized to represent the equivalent modeling approach of SWCNT-composite material in CST (MWS) software package, where this equivalent model involves the equivalent bulk material (EBM). The EBM model has the same properties of SWCNT-composite material such as effective conductivity, complex permittivity, plasma frequency, and phenomenological relaxation frequency. Therefore, by inserting these material parameters into the CST (MWS) software package, the EBM model was designed and implemented. The structure of SWCNT-composite material and EBM model are illustrated in Figure 2.

2.4. The Application of SWCNT-Composite Material

In order to estimate the electromagnetic (EM) properties of the SWCNT-composite material, the dipole antenna of EBM model was applied and solved through CST (MWS), where, the dipole antenna is considered as a simple prototype antenna adapted with this material due to the original structure of SWCNT-composite material due to the original structure of SWCNT-composite material, which is a thick rod and comprises SWCNT coated by other materials. Therefore, the equivalent modeling approach for this rod is a solid cylinder denoted by an equivalent bulk material (EBM) model.

Thus, the dipole antenna design simply has two identical arms of EBM material aligned longitudinal along the z-axis with length (L), radius ($R = r + t$) and separated by a feeding gap ($D = 2R$), as illustrated in Figure 3.

2.5. Matching Impedance of Antenna Models

The SWCNT dipole antenna is characterized by a high input impedance (Z_{insw}), based on the mathematical analysis of the SWCNT structure presented in previous research. To simplify the mathematical computation, the standard fixed impedance for microscopic antenna was ($Ro = 50\,\Omega$), whereas this value was approximate to ($Ro = 12.9\,\mathrm{k}\,\Omega$) for nano-antennas [6, 12, 30].

Mathematically, based on the antenna concepts, the surface impedance is considered as an input impedance for dipole antenna [31]. Hence, according to the equivalent circuit diagram of the SWCNT presented by Burk [8–10], the input impedance of SWCNT, which is equal to the input impedance of the equivalent nanowire model of SWCNT (σ_{equvl}) [28], is given by:

$$Z_{in,equvl} = \frac{L}{\pi\sigma_{equvl}r^2} = \frac{L}{2\pi r\sigma_{SWCNT}} \tag{19}$$

$$Z_{in,equvl} = Rq + jw\zeta \tag{20}$$

Here, Rq is the quantum resistance, and ζ is the quantum inductance. These quantities are mathematically given by:

$$Z_{in,equvl} = \frac{\pi hvL}{4e^2V_f} + jw\frac{\pi hL}{4e^2V_f} \tag{21}$$

$$Rq = \frac{\pi hvL}{4e^2V_f} = \frac{3\pi hLT}{2re^2V_f} \tag{22a}$$

$$\zeta = \frac{\pi hL}{4e^2V_f} \tag{22b}$$

$$\tag{22c}$$

With regards to the SWCNT-composite dipole antenna, the quantum resistance and quantum inductance can be estimated as presented in previous research [12, 30].

$$Z_{in,composite} = \frac{1}{2\pi r(\sigma_{composite}t)} \tag{23}$$

For simplicity, with regards to the SWCNT-composite structure, one can find the quantum parameters as given by

$$Rq = \frac{\pi hv_{composite}L}{4te^2V_f} \tag{24a}$$

$$\zeta = \frac{\pi hL}{4te^2V_f} \tag{24b}$$

One of the main problems of SWCNT dipole antenna and SWCNT-composite dipole antenna is a matching issue between these antennas and the feeding source (discreet port). In this work, the simple matching approach is presented to mitigate this problem in simulation mode. This matching approach depends on changing the Normalized Fixed Impedance (NFI) of s_{11} parameter to balance the effectiveness of the input impedance of these dipole antennas with the internal impedance of the feeding source. The NFI option of the s_{11} parameter in CST (MWS) software package is very important when the initial value of the NFI is selected based on computing the value of Rq from Equation (22a) for SWCNT or Equation (24a) for SWCNT-composite dipole antenna. This value represents the impedance value that the system is needed to realize the matching between feeding source and dipole antenna (load). In another context, this value represents a starting value to obtain an ideal value of matching impedance between source and (SWCNT or SWCNT-composite) dipole antenna to obtain the optimum result of s_{11} parameter. Indeed, the simple matching approach presented above is implemented for designing the SWCNT dipole antenna and SWCNT-composite dipole antenna. Similarly, this matching process benefits the achievement of the matching situation for different nanoelectronic antennas.

3. SIMULATION RESULTS AND DISCUSSION

In this simulation experiment, the influences of different geometrical parameters on the effective conductivity model of the SWCNT-composite material are presented. Therefore, several simulations were carried out. Also, the CST (MWS) software package was utilized to implement the equivalent modeling approaches, namely EBM for SWCNT-composite material, in order to investigate the EM properties of this material structure. Meanwhile, the NSTM for the SWCNT material was implemented to compare with the SWCNT-composite material, based on their EM properties, in which the dipole antenna configuration was employed to achieve this purpose. In the simulation experiments of this work, the radius of SWCNT is ($r = 2.7$). The discreet port was used as a feeding source for all dipole antennas designed in this work. The simulation experiments of this work can be implemented as follows.

3.1. The Investigation of SWCNT-Composite Material Properties

The simulation experiments of the effective conductivity model of SWCNT-composite material was implemented based on the mentioned Equations (9) to (13). The effect of different coating materials in this model is demonstrated in Figure 4. This simulation was implemented by testing different coating materials (i.e., copper, gold, and graphite), where an average thickness of coating layer is ($t = 2\,\text{nm}$).

The effects of changing the radius of SWCNT on the conductivity model of the SWCNT-composite materials are shown in Figure 5. The average thickness of coating layer is ($t = 2\,\text{nm}$), and the coating material is a graphite material. Meanwhile, the effects of increasing the thickness of coating layer

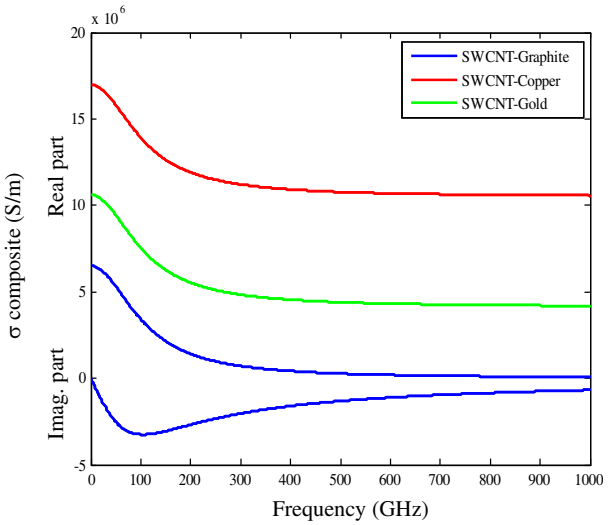

Figure 4. The effective conductivity model of the SWCNT-composite materials affected by the conductivity of different coating materials (Graphite, Copper and Gold material), at $t = 2\,\text{nm}$.

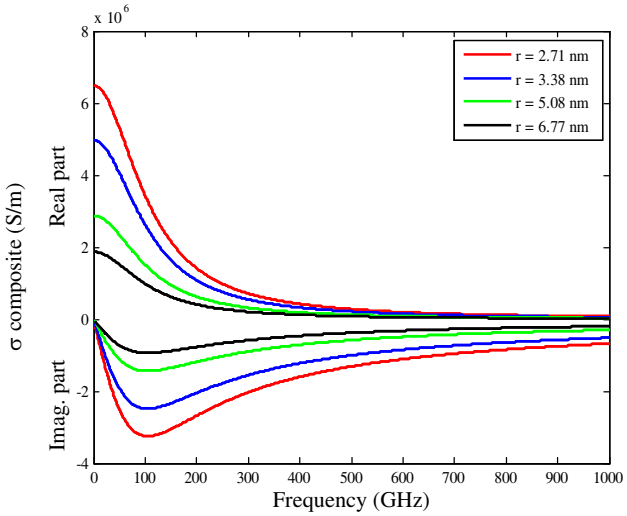

Figure 5. The effective conductivity model of the SWCNT composite material affected by several radii of SWCNT, at SWCNT coated by graphite material and the average thickness of coating layer $t = 2\,\text{nm}$.

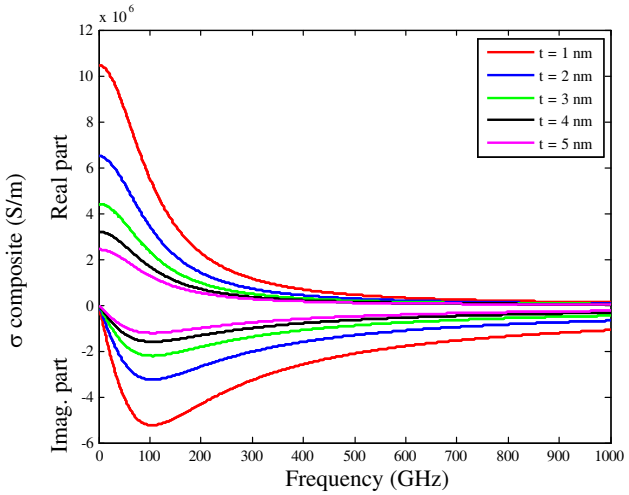

Figure 6. The effective conductivity model of the SWCNT-graphite material affected by several values of the average thickness of coating layer, at radius of SWCNT $r = 2.71\,\text{nm}$.

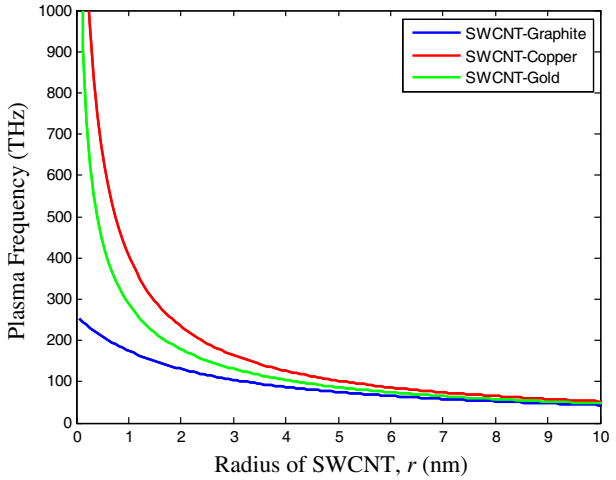

Figure 7. Plasma frequency of the SWCNT-composite materials versus the different radii of SWCNT with different type of coating materials, at average thickness of coating layer is $t = 2\,\text{nm}$.

in this conductivity model are shown in Figure 6. The radius of SWCNT is ($r = 2.71\,\text{nm}$), and the coating material is a graphite material. The behavior of the plasma frequency of the SWCNT-composite material ($W_{P,composite}$) versus different radii of the SWCNT with different types of coating materials is illustrated in Figure 7. This simulation experiment was implemented, based on a set of mentioned Equations (10) to (13).

These results show that the effective conductivity of the SWCNT-composite materials increases when SWCNT is coated by a material characterized by a high conductivity. Therefore, to obtain SWCNT-composite material with a high conductivity, the coating material characterized by a higher conductivity must be used. The effective conductivity of SWCNT-composite materials was inversely proportional for both an average thickness of coating layer and the radius of the SWCNT. The simulation results showed the dependence of the conductivity model of SWCNT-composite material on the alteration of the factors r, t, and σ_{Coat}. Meanwhile, the plasma frequency of SWCNT-composite material is affected by the conductivity of coating materials, where, this plasma frequency increases due to an increase in the conductivity of coating material.

3.2. Estimation the Electromagnetic Properties of SWCNT-Composite Material

In this simulation experiment, for the design and simulation of the SWCNT-composite dipole antenna, the EBM dipole antenna, which is equivalent to the SWCNT-composite dipole antenna, will be utilized in this work. Based on the investigation results of the SWCNT-composite material properties, the SWCNT-graphite material was adopted in this work to design the dipole antenna in the CST (MWS) software package. Therefore, the SWCNT-graphite dipole antenna was designed and implemented in different antenna lengths ($L = 10$, 20, 30, and 40) μm, based on the equivalent EBM dipole antenna. In this simulation experiment, the radius of SWCNT-graphite composite is ($R = r + t$) and separated by a feeding gap ($D = 2R$), where the average thickness of the graphite coating layer is ($t = 2\,\text{nm}$), and the radius of SWCNT is ($r = 2.71\,\text{nm}$). The simulation results of this experiment are illustrated in Figure 8 to show the s_{11} parameter for the EBM dipole antenna, and Figure 9 shows the radiation pattern for the EBM dipole antenna. Meanwhile, Figure 10 explains the directivity versus frequency for EBM dipole antenna in antenna length ($L = 30$) μm.

In order to implement the comparison between SWCNT-graphite composite material and SWCNT

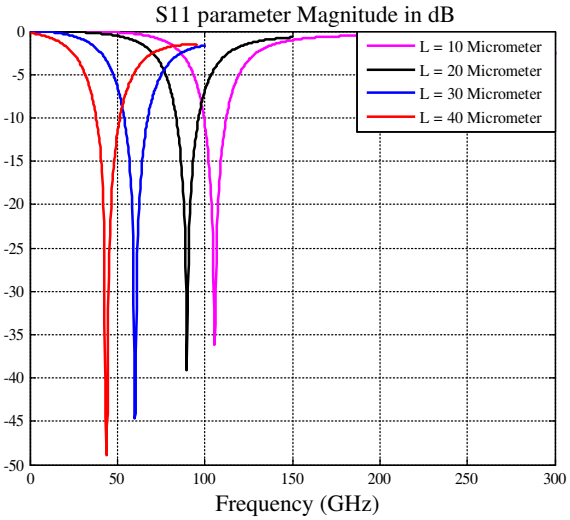

Figure 8. S_{11} parameter results of EBM dipole antenna, where the SWCNT coated by graphite material, at different antenna lengths ($L = 10$, 20, 30, and 40) μm, radius ($R = r + t$), $r = 2.71\,\text{nm}$, and $t = 2\,\text{nm}$.

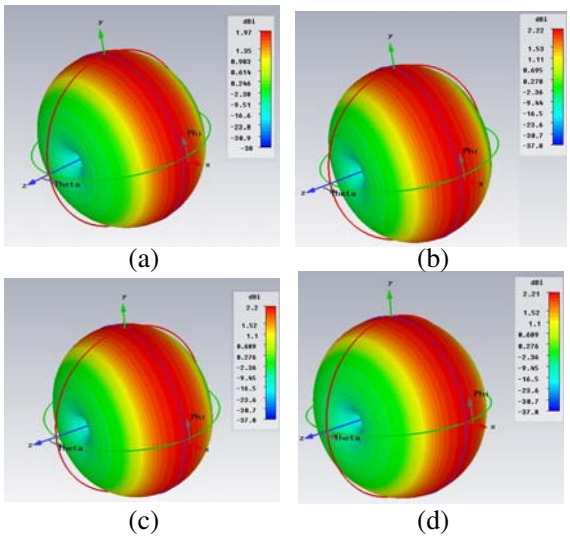

Figure 9. Radiation parameter results of EBM (SWCNT-graphite composite) dipole antenna, at different antenna lengths, (a) $L = 10$, (b) $L = 20$, (c) $L = 30$, and (d) $L = 40\,\mu\text{m}$, with radius ($R = r + t$), $r = 2.71\,\text{nm}$, and $t = 2\,\text{nm}$.

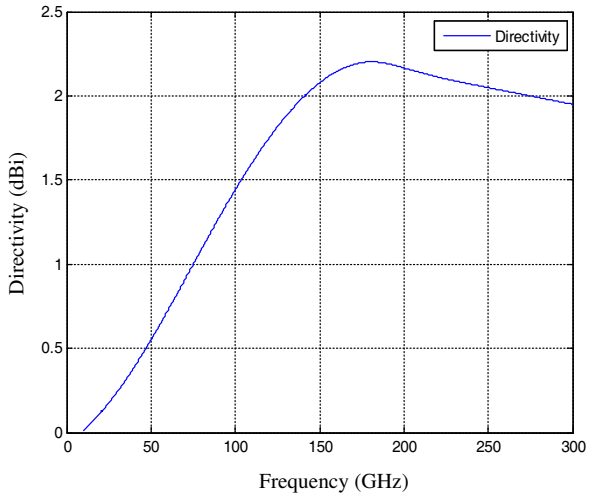

Figure 10. Directivity versus frequency for EBM dipole antenna, at antenna length $L = 30\,\mu\text{m}$, radius of SWCNT ($r = 2.71\,\text{nm}$), and $t = 2\,\text{nm}$.

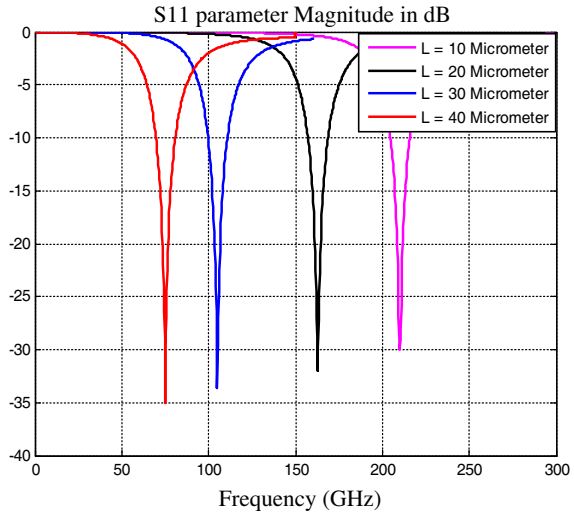

Figure 11. S_{11} parameter of NSTM dipole antenna at GHz frequency band in antenna lengths ($L = 10$, 20, 30, and $40\,\mu\text{m}$) and ($r = 2.71\,\text{nm}$).

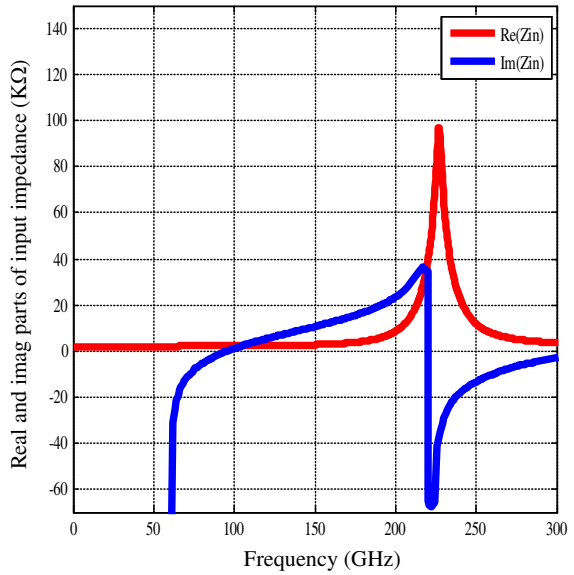

Figure 12. Input impedance of a SWCNT-graphite composite dipole antenna designed with radius $R = r + t$ and length $L = 10\,\mu\text{m}$, at $r = 2.71\,\text{nm}$, $m = 40$, and $t = 2\,\text{nm}$.

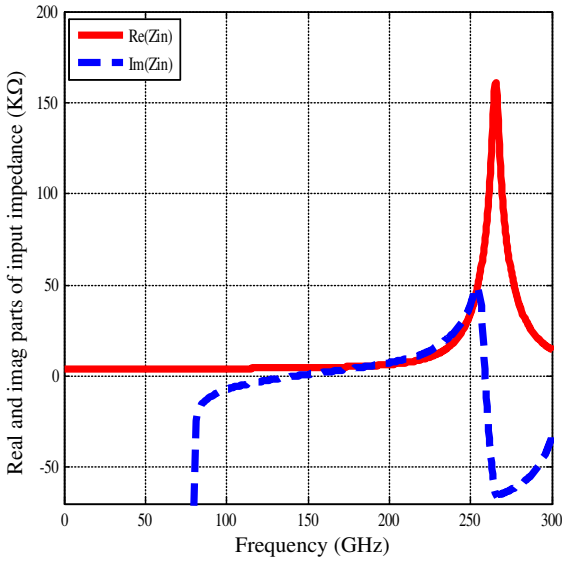

Figure 13. Input impedance of a SWCNT dipole antenna designed with radius $r = 2.71\,\text{nm}$, $m = 40$, and length $L = 10\,\mu\text{m}$.

material, the NSTM dipole antenna was designed in the CST (MWS) in antenna lengths ($L = 10$, 20, 30 and 40) μm with the radius of SWCNT is ($r = 2.71\,\text{nm}$). Figure 11 shows the s_{11} parameter for the NSTM dipole antenna with different lengths.

The simulated real and imaginary parts of the input impedance of EBM (SWCNT-graphite composite) dipole antenna are shown in Figure 12. This dipole antenna is designed with radius ($R = r + t$) and length $L = 10\,\mu\text{m}$, at $r = 2.71\,\text{nm}$, $m = 40$, and $t = 2\,\text{nm}$. The resonant frequency occurs at 100.5 GHz, a travelling point from the capacitance to the inductance properties. Similarly, the simulated input impedance of NSTM (SWCNT) dipole antenna is shown in Figure 13. This dipole

antenna was designed with radius $r = 2.71\,\text{nm}$, $m = 40$ and length $L = 10\,\mu\text{m}$. The resonant frequency occurs at 210 GHz.

The effect of different radii (R) on the behavior of the EBM dipole antenna is illustrated in Figure 14 with antenna length ($L = 10\mu\text{m}$). The radius (R) changes based on a change of the value of index integer (m), which leads to change of the radius of SWCNT. Meanwhile, the effect of different radii (R) on the behavior of the EBM dipole antenna is illustrated in Figure 15. At antenna length ($L = 10\,\mu\text{m}$) and radius of SWCNT ($r = 2.71\,\text{nm}$), the radius (R) changes based on the change in the average thickness of coating layer (t).

By comparing the results of SWCNT dipole antenna and SWCNT-graphite composite dipole antenna from Figure 8 and Figure 11, the improvement is indicated for the s_{11} parameter after coating the SWCNT by a thin layer of graphite material. Meanwhile, the resonant frequencies were reduced due to the same reason. These comparisons are implemented based on the equivalent modeling approaches for both material structures (SWCNT and SWCNT-graphite composite material). Figure 14 and Figure 15 show a significant increase in the radius of SWCNT-composite material, which leads to a redaction of the resonant frequencies of this composite dipole antenna. Table 1 presents a summary of the results of this comparison.

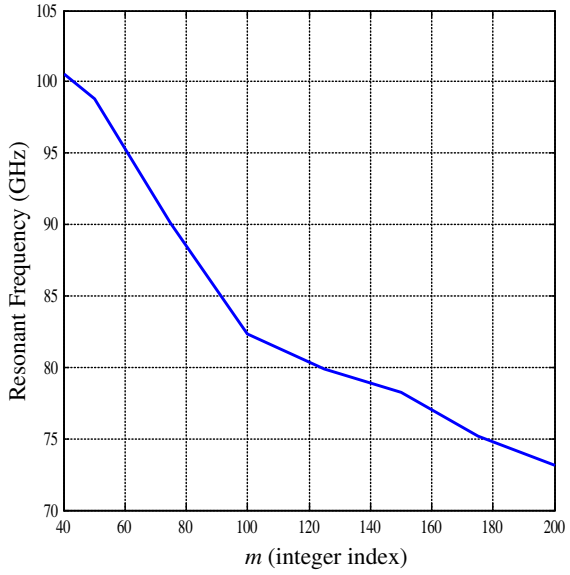

Figure 14. Resonant frequency versus m index integer of SWCNT, at EBM (SWCNT-graphite composite) dipole antenna length ($L = 10$) μm.

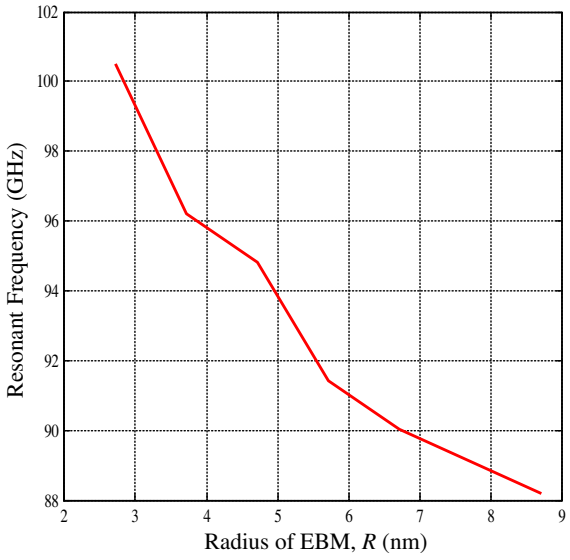

Figure 15. Effect the changing of the average coating layer on the behaviorof the EBM (SWCNT-graphite composite) dipole antenna, at antenna length ($L = 10$) μm and radius of SWCNT ($r = 2.71\,\text{nm}$).

Table 1. Summary results of SWCNT and SWCNT-graphite composite dipole antennas.

L (μm)	Fr SWCNT (GHz)	Fr SWCNT-graphite composite (GHz)	S_{11} parameter SWCNT (dB)	S_{11} parameter SWCNT-graphite composite (dB)
10	210	100.5	−30	−36.2
20	162	89.7	−32	−39.04
30	105	60	−33	−44.6
40	76	43.7	−35	−48.9

Also, the bandwidth (BW) and fractional bandwidth (FBW) are improved at the SWCNT-graphite composite dipole antenna compared with the SWCNT dipole antenna. As can be seen from Figure 9 and Figure 10, the directivity of the SWCNT-graphite composite dipole antenna remains the same in the range of the acceptable standard value. These results lead to making the SWCNT-graphite composite dipole antenna operate with a high data rate, compared with the SWCNT dipole. Table 2 exhibits the summary results of the comparison of the BW and FBW for both dipole antennas with different antenna lengths.

Table 2. Summary results of BW and FBW for SWCNT and SWCNT-graphite composite dipole antennas.

L (μm)	***BW* SWCNT (GHz)**	**BW SWCNT-graphite composite (GHz)**	**FBW SWCNT (%)**	**FBW SWCNT-graphite composite (%)**
10	11.302	14.1	5.34	15.3
20	11.551	14.532	8.217	16.51
30	11.626	14.844	14.5	24.1
40	12.201	15.110	14.8	25.3

4. CONCLUSIONS

In this paper, the mathematical analysis for the SWCNT-composite material was presented for antenna applications. The key material parameters of this composite material were estimated such as effective conductivity, relative complex permittivity plasma frequency, and phenomenological relaxation frequency. The effective conductivity and other parameters of the SWCNT-composite material were affected by the factors r, t, and σ_{Coat}. Hence, the new composite material has unique properties which are dependent on the properties of both SWCNT and coating material. Based on these parameters, an efficient modeling approach for the SWCNT-composite material was presented and implemented in the CST (MWS) software package, where the SWCNT-composite material is SWCNT coated by a thin layer of other materials. Also, the simple modeling approach for SWCNT was presented and implemented in CST (MWS) software package, to compare with the SWCNT-composite dipole antenna. The SWCNT-graphite composite material structure was adopted in this work, due to its properties compared with the other SWCNT-composite materials. The modeling approaches were used to investigate the EM properties of these materials based on the dipole antenna configuration. For the simulation purpose, the required mathematical analysis was also presented in order to support these modeling approaches.

Finally, the comprehensive EM comparisons between SWCNT-graphite composite material and SWCNT material were also presented. From these comparisons, the EM performance enhancement for the SWCNT-graphite composite dipole antenna is demonstrated. Therefore, in the future work, it is proposed that the bundle of SWCNT-graphite composite material should be utilized for the design of more efficient dipole antenna.

REFERENCES

1. Wood, J. R. and H. D. Wagner, "Single-wall carbon nanotubes as molecular pressure sensors," *Appl. Phys. Lett.*, Vol. 67, 2883–2885, 2000.
2. Li, C. Y. and T. W. Chou, "Strain and pressure sensing using single-walled carbon nanotubes," *Nanotechnology*, Vol. 15, 1493–1496, 2004.
3. Li, J., Y. Lu, Q. Ye, M. Cinke, J. Han, and M. Meyyappan, "Carbon nanotube sensors for gas and organic vapor detection," *Nano Lett.*, Vol. 3, 929–933, 2003.
4. Besteman, K., J.-O. Lee, F. G. M. Wiertz, H. A. Heering, and C. Dekker, "Enzyme-coated carbon nanotubes as single-molecule biosensors," *Nano Lett.*, 727–730, 2003.

5. Hoenlein, W., F. Kreupl, G. S. Duesberg, A. P. Graham, M. Liebau, R. V. Seidel, and E. Unger, "Carbon nanotube applications in microelectronics," *IEEE Trans. on Components and Packaging Tech.*, Vol. 27, 629–634, 2004.
6. Hanson, G. W., "Fundamental transmitting properties of carbon nanotube antennas," *IEEE Transactions on Antenna and Propagation*, Vol. 53, 3426–3435, 2005.
7. Hanson, G. W. and J. A. Berres, "Multiwall carbon nanotubes at RF-THz frequencies: Scattering, shielding, effective conductivity and power dissipation," *IEEE Transactions on Antenna and Propagation*, Vol. 59, 3098–3103, 2011.
8. Burke, P. J., "Lüttinger theory as a model of the gigahertz electrical properties of carbon nanotubes," *IEEE Transaction on Nanotechnology*, Vol. 1, 129–144, 2002.
9. Burke, P. J., "Correction to Lüttinger liquid theory as a model of the gigahertz electrical properties of carbon nanotubes," *IEEE Transaction on Nanotechnology*, Vol. 3, 331, 2004.
10. Burke, P. J., "An RF circuit model for carbon nanotubes," *IEEE Transaction on Nanotechnology*, Vol. 2, 55–58, 2003.
11. Burke, P. J., "Correction to an RF circuit model for carbon nanotubes," *IEEE Transaction on Nanotechnology*, Vol. 3, 331, 2004.
12. Burke, P., S. Li, and Z. Yu, "Quantitative theory of nanowire and nanotube antenna performance," *IEEE Transaction on Nanotechnology*, Vol. 5, 314–334, 2006.
13. Hanson, G. W. and J. Hao, "Infrared and optical properties of carbon nanotube dipole antennas," *IEEE Transaction on Nanotechnology*, Vol. 5, 766–775, 2006.
14. Hanson, G. W., "Current on an infinitely-long carbon nanotube antenna excited by a gap generator," *IEEE Transaction on Antennas and Propagation*, Vol. 54, 76–81, 2006.
15. Arash, B., Q. Wang, and V. K. Varadan, "Mechanical properties of carbon nanotube/polymer composites," *Scientific Reports*, Vol. 4, Article Number 6479, 1–8, 2014.
16. Chu, K. and S.-H. Park, "Fabrication of a hybrid carbon-based composite for flexible heating element with a zero temperature coefficient of resistance," *IEEE Electron Device Letters*, Vol. 36, 50–52, 2015.
17. Fan, J., Z. Chen, N. Tang, H. Li, and Y. Yin, "Supercapacitors based on composite material of MnO_2 and carbon nanotubes," *Proceedings of the 13th IEEE International Conference on Nanotechnology Beijing*, 933–963, China, 2013.
18. Aryasomayajula, L., R. Rieske, and K.-J. Wolter, "Application of copper-carbon nanotubes composite in packaging interconnects," *34th Int. Spring Seminar on Electronics Technology*, 531–536, 2011.
19. Bakrudeen, S. B., "Dramatic improvement in mechanical properties and sem image analysis of AI-CNT composite," *Proceedings of the International Conference on Advanced Nanomaterial & Emerging Engineering Technologies (ICANMEET-20J3)*, 184–189, 2013.
20. Han, W.-Q. and A. Zettl, "Coating single-walled carbon nanotubes with tin oxide," *Nano Lett.*, Vol. 3, 681–683, 2003.
21. Li, H., C.-S. Ha, and II Kim, "Fabrication of carbon nanotube/SiO_2 and carbon nanotube/SiO_2/Ag nanoparticles hybrids by using plasma treatment," *Nanoscale Res. Lett.*, Vol. 4, 1384–1388, 2009.
22. Su, Y., H. Wei, Z. Yang, and Y. Zhang, "Highly compressible carbon nanowires synthesized by coating single-walled carbon nanotubes," *Carbon*, Vol. 49, 3579–3584, 2001.
23. Qunqinq, L., S. Fan, W. Han, C. H. Sun, and W. Liang, "Coating of carbon nanotube with nickel by electroless plating method," *Jpn. J. Appl. Phys.*, Vol. 36, L501–L503, 1997.
24. Zhu, L., G. Lu, S. Mao, and J. Chen, "Ripening of silver nanoparticles on carbon nanotubes," *Nano: Brief Rep. and Rev.*, Vol. 2, 149–156, 2007.
25. Morihisa, Y., C. Kimura, M. Yukawa, H. Aoki, T. Kobayashi, S. Hayashi, S. Akita, Y. Nakayama, and T. Sugino, "Improved field emission characteristic of individual carbon nanotube coated with boron nitride nanofilm," *J. Vac. Sci. Technol. B*, Vol. 26, 872–875, 2008.
26. Peng, Y. and Q. Chen, "Fabrication of one-dimensional Ag/multiwalled carbon nanotube nanocomposite," *Nanoscale Res. Lett.*, Vol. 7, 1–5, 2012.

27. Peng, Y. and Q. Chen, "Fabrication of copper/MWCNT hybrid nanowires using electroless copper deposition activated with silver nitrate," *J. Electrochen Soc.*, Vol. 159, D72–D76, 2012.
28. Hanson, G. W., "A common electromagnetic framework for carbon nanotubes and solid nanowires-spatially distributed impedance, and transmission line model," *IEEE Transaction on Microwave Theory and Techniques*, Vol. 59, 9–20, 2011.
29. Orfanidis, S. J., "Electromagnetic waves and antennas," *Maxwell's Equations*, Chapter 1, 2010.
30. Hanson, G. W., "Radiation efficiency of nanoradius dipole antennas in the microwave and far-infrared regime," *IEEE Antenna and Propagation Magazine*, Vol. 50, 1–10, 2008.
31. Balanis, C. A., *Antenna Theory Analysis and Design*, 3rd Edition, John Wiley and Sons, USA, 2005.